TECHNICAL PAPER

ISSN 1047-3289 *J. Air & Waste Manage. Assoc.* **55**:1085–1099

Control of Ozone Precursors in a Complex Industrial Terrain by Using Multiscale-Nested Air Quality Models with Fine Spatial Resolution (1 km^2)

Pedro Jiménez, René Parra, and José M. Baldasano

Laboratory of Environmental Modeling, Universitat Politècnica de Catalunya, Barcelona, Spain

ABSTRACT

The location of the northeastern Iberian Peninsula (NEIP) in the northwestern Mediterranean basin, the presence of the Pyrenees mountain range (with altitudes >3000 m), and the influence of the Mediterranean Sea and the large valley canalization of Ebro river induce an extremely complicated structure for the dispersion of photochemical pollutants. Air pollution studies in very complex terrains such as the NEIP require high-resolution modeling for resolving the very complex dynamics of flows. To deal with the influence of larger-scale transport, however, high-resolution models have to be nested in larger models to generate appropriate initial and boundary conditions for the finer resolution domains. This article shows the results obtained through the utilization of the MM5-EMICAT2000-CMAQ multiscale-nested air quality model relating the sensitivity regimes for ozone (O_3)-nitrogen oxides (NO_x)-volatile organic compounds (VOCs) in an area of high geographical complexity, like the industrial area of Tarragona, located in the NEIP. The model was applied with fine temporal (one-hour) and spatial resolution (cells of 24 km, 2 km, and 1 km) to represent the chemistry and transport of tropospheric O_3 and other photochemical species with respect to different hypothetical scenarios of emission controls and to quantify the influence of different emission sources in the area. Results indicate that O_3 chemistry in the industrial domain of Tarragona is strongly sensitive to VOCs; the higher percentages of reduction for ground-level O_3 are achieved when reducing by 25% the emissions of industrial VOCs. On the contrary, reductions in the industrial emissions of NO_x contribute to a strong increase in hourly peak levels of O_3. At the same time, the contribution of on-road traffic and biogenic emissions to ground-level O_3 concentrations in the area is negligible with respect to the pervasive weight of industrial sources. This analysis provides an assessment of the effectiveness of different policies for the control of emission of precursors by comparing the modeled results for different scenarios.

IMPLICATIONS

A multiscale-nested approach was applied in order to being able to simulate photochemical pollution in very complex terrains, as the NEIP, and, more specifically, the industrial domain of Tarragona. The study of different scenarios indicate that air quality modeling could be a useful tool to evaluate the chemical sensitivity of the system O_3-NO_x-VOCs when establishing policies of emissions controls from different emitter sources, specially from industrial and traffic sources.

INTRODUCTION

The northeastern Iberian Peninsula (NEIP) is located in the northwestern Mediterranean basin and has a very complex topography. The complex configuration of the zone is affected by the presence of the Pyrenees mountain range (with altitudes >3000 m), the influence of the Mediterranean Sea, and the large valley canalization of the Ebro river (Figure 1). The relief of the NEIP is organized in three structural units forming a fan-shape formation with the vertex in the Empordà: (1) the Pyrenees, forming a barrier at the north of the region and expanding from east to west, constitute the first great unity; (2) the Central Depression stretches through all interior zones, from la Plana de Vic until the vast plains of Pla de Lleida; and (3) the Mediterranean System, formed by the joint of coastal mountain ranges and depressions parallel to the coast, extending from Cap de Begur until Montsià.

The complex topography of the NEIP induces an extremely complicated structure of the flow because of the development of α- and β-mesoscale phenomena that interact with synoptic flows. The characteristics of the breezes have important effects in the dispersion of pollutants. In addition, the flow can be even more complex because of the nonhomogeneity of the terrain, the land use, and the types of vegetation. In these situations, the structure of the flow is extremely complicated because of the superposition of circulations of different scale.

Therefore, air pollution studies in very complex terrains like the NEIP require high-resolution modeling of air

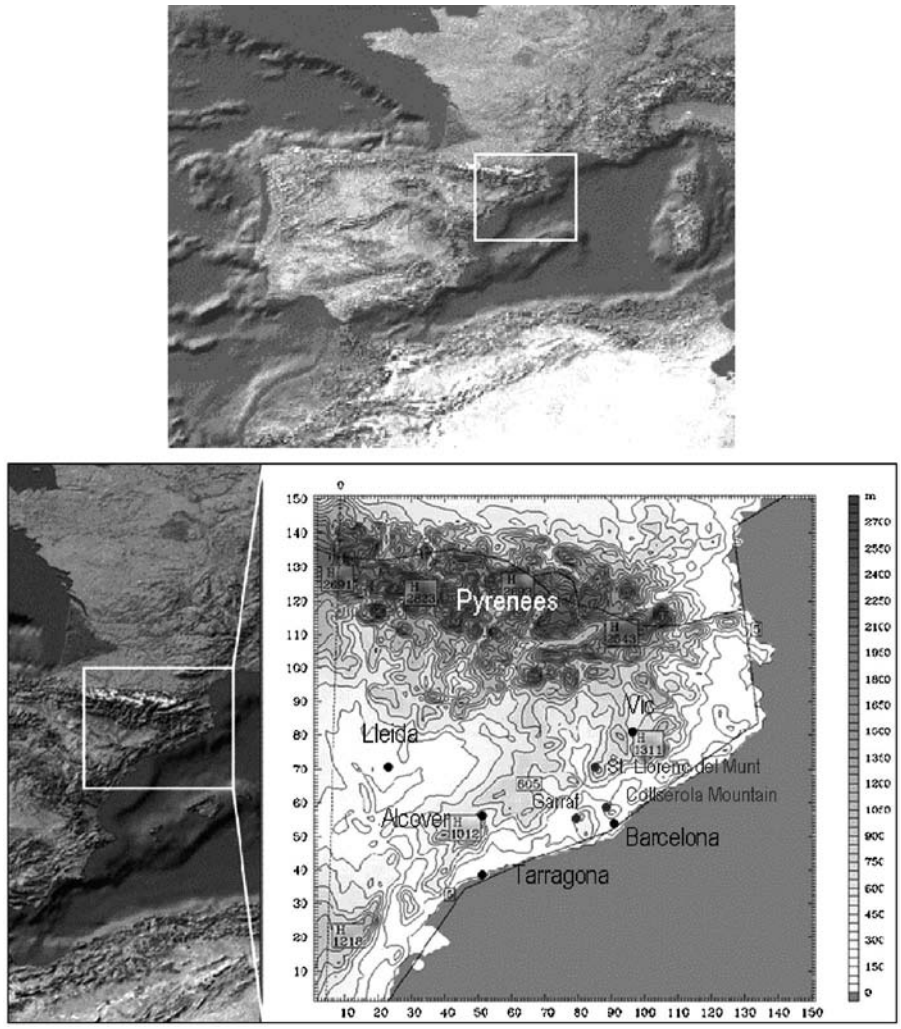

Figure 1. Location of the NEIP in the Western Mediterranean Basin, relief, and main geographical features.

quality (with a resolution of ≤1 km) for resolving very complex structures, such as flow channeling in valleys or the influence of line and point sources.[1,2] To deal with the influence of larger-scale transport, however, high-resolution models have to be nested in larger models (i.e., treating larger areas with lower resolution) to generate appropriate initial and boundary conditions for the finer resolution domains.

The kinetics of ozone (O_3) chemistry and its two main precursors, nitrogen oxides (NO_x) and volatile organic compounds (VOCs), represent an important source of uncertainty in atmospheric chemistry and photochemical modeling.[3] It is generally known that under some conditions, O_3 concentrations increase with increasing NO_x and are largely insensitive to VOC, whereas for other conditions the rate of formation will increase with increasing VOC and will be unchanged or decrease with increasing NO_x.

This complexity affects the design of control strategies to reduce tropospheric O_3 production. Nowadays, considerable interest exists in finding observable indicators of how real air masses are likely to respond to emission controls. A major problem for the study of O_3-NO_x-VOC sensitivity has been the inability to gain evidence based on direct measurements rather than theoretical calculations,[4] and, therefore, air quality models are a useful tool to establish policies for controlling the emissions of the species that act as precursors of tropospheric O_3.

This work shows the results obtained through the utilization of the MM5-EMICAT2000-CMAQ multiscale-nested air quality model relating the sensitivity regimes for O_3-NO_x-VOCs in an area of high geographical complexity, like the industrial area of Tarragona, located in the NEIP. The main emission sources in the NEIP are located on an axis parallel to the coast, especially in the Barcelona Geographical Area and the Tarragona industrial zone. This latter area contains very important industrial sources, such as two refineries, several chemical complexes, and cogeneration power plants and incinerators, among others. The air quality model was applied with fine temporal and spatial resolution to represent the chemistry and transport of tropospheric O_3 and other photochemical

species with respect to different hypothetical scenarios of emission controls. This analysis provides an assessment of the effectiveness of different policies for the control of emission of precursors by comparing the modeled results for different scenarios.

METHODS

Modeling results are based on a photochemical pollution event in the Western Mediterranean Basin that took place on August 13–16, 2000. Simulation shows the results for August 15, 2000, which is a representative day of this episode. Values around the European threshold of 180 $\mu g\ m^{-3}$ for tropospheric O_3 are attained in different locations in the NEIP. Meteorologically, the episode is characterized by a low pressure gradient (Figure 2) that allows the development of mesoscale phenomena. Weak northwestern winds are observed aloft. The sea breeze and the complex topography of the area produce important orographic injections because of mechanical and thermal convection processes.[5] These situations are associated with typical summertime recirculation episodes with high concentrations of photochemical pollutants, such as O_3 and both primary and secondary particulate matter. This modeled episode is representative of meteorological situations in the Western Mediterranean Basin, because the occurrence of regional recirculations at low levels represents 45% of the yearly flow transport patterns over the area of study and >70% of summer transport patterns.[6] The limitation of external air mass inflows in the area during the episode (because of meteorological limitations) minimizes the influence of boundary conditions on maximum pollutants concentrations that are influenced mainly by local photochemistry.

The complex configuration of the NEIP produces a sharp gradient in its characteristics and forces to the use of complex multiscale-nested models with very high resolution to generate properly the initial and boundary conditions in the area of study. Therefore, three different

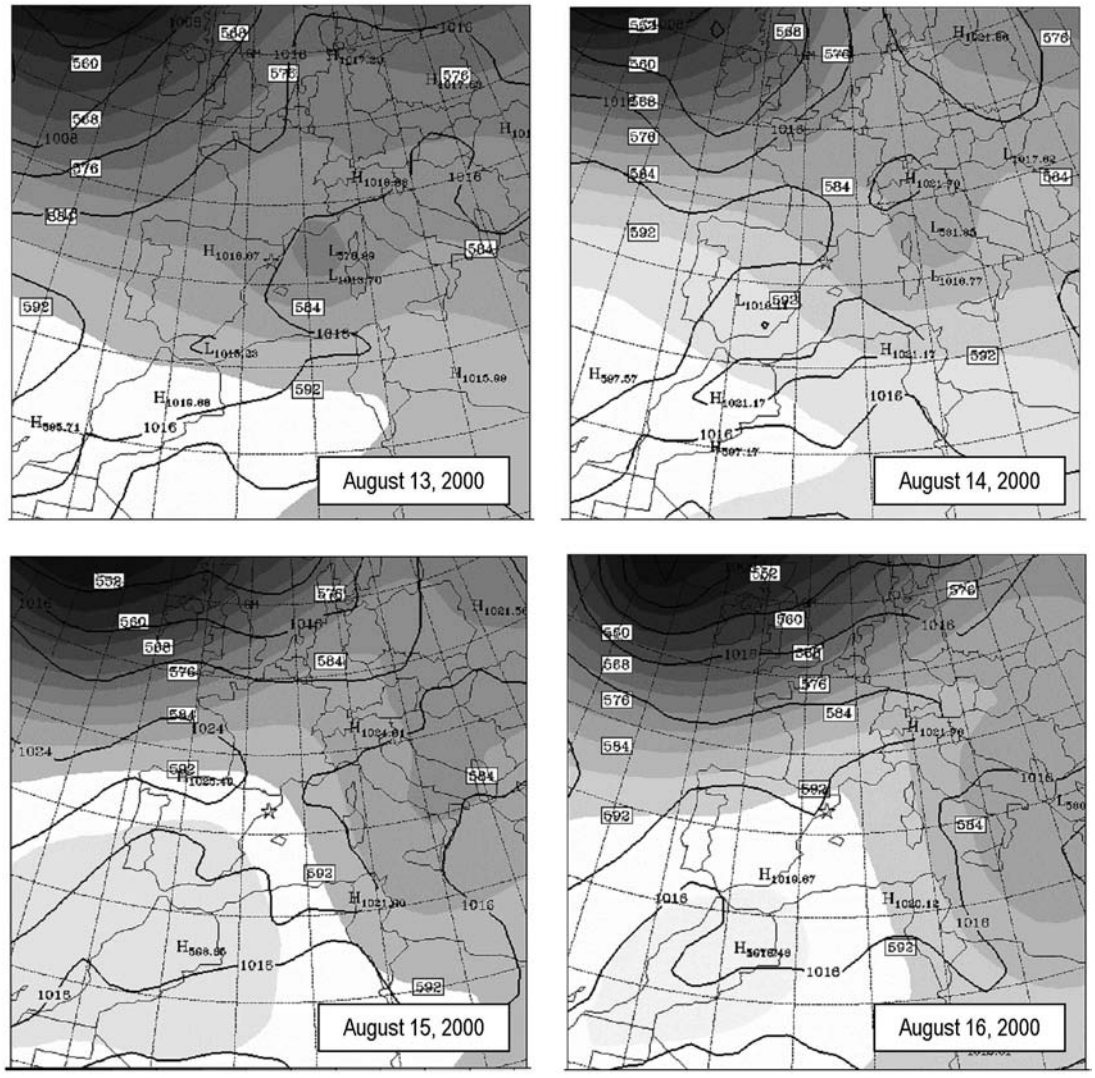

Figure 2. Synoptic situation of August 13, 2000 to August 16, 2000 (shaded map: 0000 UTC 500 HPA analysis, contour map: 0000 UTC surface analysis).

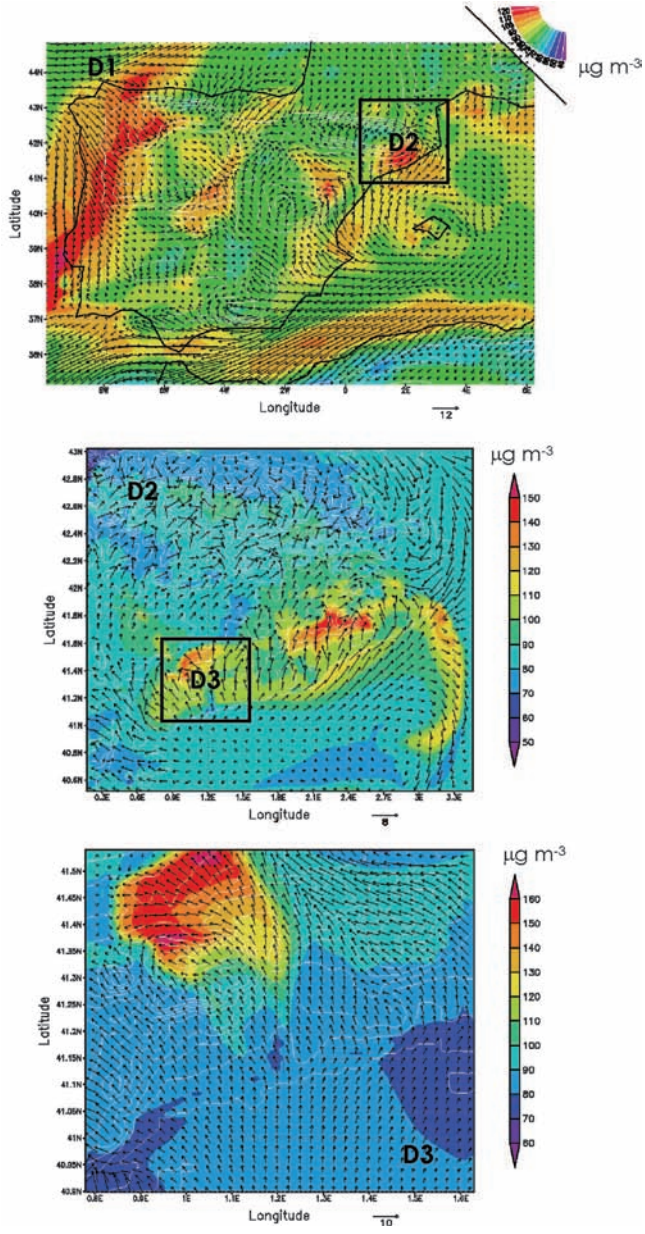

Figure 3. Ozone (μg m^{-3}) results for different nested domains at 1200 UTC on August 15, 2000: Peninsular domain (D1, up); northeastern Iberian Peninsula (D2, center); and Tarragona (D3, down).

nested domains were defined for performing simulations (Figure 3). The first was a 1392 × 1104 km^2 domain (D1) centered in the Iberian Peninsula, that covers the Iberian Peninsula, northern Africa, and the western Mediterranean Basin with a horizontal resolution of 24 km and 16 vertical layers in σ-coordinates (having the first layer at an altitude ~36 m above ground level). Emissions of this domain were obtained from European Monitoring and Evaluation Programme data for the year 2000 (http://www.emep.int). The second was a 272 × 272 km^2 domain (D2) covering the NEIP with a horizontal resolution of 2 km and identical vertical resolution. The third was a 40 × 40 km^2 domain (D3) centered in the city of Tarragona that covers the industrial complex around this city with a horizontal resolution of 1 km and 16 vertical layers covering the troposphere. Emissions for D2 and D3 were generated with the EMICAT2000 emission model.[7] Figure 3 shows a first approximation to the lack of detail obtained when applying coarser horizontal resolutions.

Models

The MM5 numerical weather prediction model[8] provided the meteorology dynamical parameters. MM5 physical options used for the simulations were: Mellor-Yamada scheme as used in the Eta model for the PBL parameterization; Anthes-Kuo and Kain-Fritsch cumulus scheme; Dudhia simple ice moisture scheme; the cloud-radiation scheme; and the five-layer soil model. Initialization and boundary conditions for the mesoscale model were introduced with analysis data of the European Center of Medium-range Weather Forecasts global model. Data were available at a 1-degree resolution (~100-km at the working latitude) at the standard pressure levels every six hours.

The high-resolution (1 hr and 1 km^2) EMICAT2000 emission model has been applied in the NEIP. As precursors of photochemical smog, the model estimates the cell emissions of NO_x, nonmethane VOCs (NMVOCs), CO, and also total suspended particles and sulfur dioxide (SO_2). This emission model includes the emissions from vegetation, on-road traffic, industries, and emissions by fossil fuel consumption and domestic-commercial solvent use. Biogenic VOC emissions were estimated using a methodology that takes into account local vegetation data (land-use distribution and biomass factors) and meteorological conditions (surface air temperature and solar radiation) together with emission factors for native Mediterranean species and cultures.[9] On-road traffic emission includes the hot exhaust, cold exhaust, and evaporative emissions using the methodology and emission factors of the European model EMEP/CORINAIR–COPERTIII[10] as the basis and differentiating the vehicle park composition between weekdays and weekends.[11] Industrial emissions include real records of some stacks connected to the emission control net of the Environmental Department of the Catalonia Government and the estimated emissions from power stations (conventional and cogeneration units), incinerators, cement factories, refineries, olefin plants, and chemical industries.

The chemical transport model used to compute the concentrations of photochemical pollutants was Models-3/CMAQ.[12] A 48-hr spin-up was performed to minimize the influence of initial conditions.[13] According to the results of Jiménez et al.,[14] the chemical mechanism selected for simulations was CBM-IV,[15] including aerosols and heterogeneous chemistry. The algorithm chosen for

the resolution of tropospheric chemistry was the Modified Euler Backward Iterative method.[16]

Hypothesis for the Control of Precursors

The Gothenburg Protocol and the Directive 2001/81/EC[17] were adopted to abate the acidification, eutrophication, and ground-level O_3 and to set national emission ceilings for certain atmospheric pollutants. These documents established emission limits for the year 2010 for different photochemical species (NO_x, VOCs and sulfur compounds, among others), and the reductions set for the O_3 precursors are considered with respect to the reference year of 1990: 41% in the case of NO_x, 40% in the case of VOCs, and 63% for SO_2. If we focus in O_3 precursors, reductions of 27% are achieved for NO_x and VOCs during the period 1990[18]–2000[7] in the case of the NEIP; therefore, reductions around 20% are needed to agree with the hypothesis of the Gothenburg Protocol and Directive 2001/81/EC (Table 1).

Considering that most of the industrial emissions in the NEIP are located in the area of Tarragona (D3) and that these industries in D3 do not exhibit a considerable seasonal fluctuation in their emissions,[7] hypothetical uniform reductions during the entire year have been considered for setting control policies of industrial sources in the zone of Tarragona and to assess their effect in the sensitivity regimes of O_3-NO_x-VOCs. The effects in the air quality of this area were evaluated for the following scenarios: (1) base case: for year 2000 with emissions estimated by EMICAT2000 (vegetation, traffic, industrial emissions, and also associated to the domestic and commercial use of solvents and fossil fuels); (2) scenario 1: reduction of 25% in the industrial emissions of nitrogen oxides emissions in the area of Tarragona (D3); (3) scenario 2: reduction of 25% in the industrial emissions of VOCs in the area of Tarragona (D3); (4) scenario 3: reduction of 25% in the industrial emissions of both nitrogen oxides and VOCs in the area of Tarragona (D3); (5) scenario 4: reduction of 50% in the emissions derived from on-road traffic in the area of Tarragona (D3); (6) scenario 5: reduction of 100% in the emissions of the refinery located in D3; and (7) furthermore, to estimate the contribution of biogenic emissions in this domain, an additional scenario was included (scenario 6: reduction of 100% in biogenic emissions in D3).

Table 1. Emissions (kt yr^{-1}) of NO_x, VOCs, and SO_2 in Catalonia for 1990[18] and 2000[7] and objectives to achieve in year 2010.

	NO_x	VOCs	SO_2
Year 1990	147.3	136.6	116.6
Year 2000	106.9	99.3	64.7
Objective 2010	86.9	82.0	43.1
Reduction 1990–2000	27.4%	27.3%	56.0%
Required reduction 2000–2010	18.7%	17.4%	33.4%

Table 2. Summary of emissions in the NEIP for the base case (%) in year 2000.

	Primary Pollutants (%)					
Source	**NO_x**	**NMVOCs**	**CO**	**SO_2**	**TSP**	**Total**
Biogenic emissions		34.33				7.83
On-road traffic	58.37	36.24	96.86	2.01	66.81	64.75
Industrial emissions	38.54	16.69	2.73	94.44	31.91	23.35
Power generation	14.03	0.51	0.79	44.05	7.23	8.01
Cement factories	8.98	0.22	1.31	2.16	17.87	3.17
Refining	7.95	4.69	0.41	38.64	3.83	6.99
Olefins	2.71	1.76	0.00	9.58	2.98	2.04
Fugitive emissions		8.05				1.84
Others	4.86	1.46	0.22	0.00	0.00	1.30
Energetic consume domestic & commercial	3.09	0.15	0.41	3.55	1.28	1.20
Use of solvents		12.59				2.87
Total	100	100	100	100	100	100

Base Case Emissions

The main emission sources in the NEIP (D2) are located on the coast, especially in the Barcelona geographical area and the Tarragona industrial zone. The importance of biogenic emissions is high in D2, representing a 34% of total annual VOCs emissions, and are a source of reactive compounds, such as aldehydes, terpenes, and isoprene.[7] Traffic emissions on an annual cycle represent 58% of the emissions of NO_x and 36% of VOCs in D2, especially olefins and aromatic compounds. On August 15, 2000, emissions had an additional weight, because traffic increased because of the vacation period and the contribution of foreign vehicles. Main emitters are located in the axis of roads parallel to the coast and the cities of Barcelona and Tarragona. Industrial emissions are located mainly in D3 and represent 39% of the emissions of NO_x and 17% of the emissions of VOCs; meanwhile, the domestic and commercial use of solvents represents 13% of the VOCs emissions in D2.[7] The emission of precursors attributable to the industrial sector in the NEIP add up to 41 kt yr^{-1} of NO_x and 23 kt yr^{-1} of VOCs. In the annual cycle, total emissions of O_3 precursors in D2 are 106.9 kt yr^{-1} of NO_x (58% traffic emissions, 39% industrial emissions) and 99.3 kt yr^{-1} of NMVOCs (34% biogenic emissions, 36% on-road traffic emissions, and 17% industrial emissions). Total percentage of the contribution of different sources to total emissions in D2 are summarized in Table 2.

Table 3. RMS error statistic of wind speed and wind direction at 0000, 1200, and 2400 UTC for August 13–16, 2000 (surface values evaluated with 52 surface stations, aloft values evaluated with a radiosonde).

	00 UTC	12 UTC	24 UTC
RMSE Wind speed (m/sec)			
Surface 10 m	1.71	2.04	2.00
Radio. <1000 m	0.84	1.04	1.31
1000—5000 m	5.03	1.55	3.7
5000—10,000 m	8.45	5.15	3.94
RMSE Wind direction (°)			
Surface 10 m	95.95	44.74	89.40

Emissions of O_3 precursors on August 15, 2000, were 236 t day^{-1} for nitrogen oxides and 172 t day^{-1} for VOCs. The ratio NO_x:NMVOCs that is 0.78 for the annual cycle decreases to 0.58 for this episode of photochemical pollution because of the high temperatures and solar radiation that promote evaporative emissions from on-road traffic and vegetation. Most of the anthropogenic emissions derived from on-road traffic and the domestic sector are located in the Barcelona geographical area and in the axis of the highways oriented parallel to the coastline. Industrial emissions are located principally in D3, in the industrial area of Tarragona, where there are two refineries, several chemical complexes, cogeneration power plants, and incinerators, among others. In this D3, EMICAT2000 estimates a total of 15.7 kt yr^{-1} of NO_x and 20.2 kt yr^{-1} of NMVOCs from industrial activities. These values represent 15% of total emissions in the NEIP (D2). Industrial emissions of NO_x and VOCs in D3 represent 38% and 88%, respectively, of the total industrial emissions in D2. In the case of the refinery, the most important industrial source in D3, annual emissions of O_3 precursors, are 7.2 kt yr^{-1} of NO_x and 5.3 kt yr^{-1} of NMVOCs.

RESULTS AND DISCUSSIONS

Evaluation of Nested Domains

The precise definition of the grid resolution is an important decision when applying an air quality model. Jiménez et al.[1] showed that O_3 is highly sensitive to the grid size used in the simulations, and very high spatial and temporal resolution is needed to capture the small-scale features in very complex terrains.

Meteorological model has been evaluated comparing model results with surface and aloft wind measurements. Validation data of 52 surface stations located across the domain and a radiosonde launched in Barcelona (in the center of the domain in the coast) were used. For meteorological fields, Table 3 shows the root mean square (RMS) error of wind speed at 10 m for the lower, middle, and upper troposphere and RMS error of wind direction (10 m) at 0000, 1200, and 2400 Coordinate Time Universal (UTC). The general behavior of the model shows a tendency to overestimate nocturnal surface winds and to underestimate the diurnal flow. A clear improvement is produced in the simulation during the central part of the day; at this time, the complex structure of the sea breeze described by simulation and the development of up-slope winds appears to agree in a higher grade with surface measurements. The statistics show how the model presents a better behavior within the boundary layer, and major disagreement with the radiosonde appears >1000 m above ground-level.

Air quality stations hourly data averaged over the domain of study were used to report the difference in the forecasted O_3 levels for the base case with the different nested domains and their performance results. Hourly values of ground-level O_3 were provided by 48 air quality surface stations in northeastern Spain, which belong to the Environmental Department of the Catalonia Government (Spain). Despite the fact that surface measurements represent values only at a given horizontal location and height, whereas the concentration predicted by the model represents a volume-averaged value, ground-level O_3 results were statistically evaluated by comparing the first-layer simulations results and the values measured in the air quality stations of the domain under study. Therefore, the maximum simulated value in the domain (182 $\mu g\ m^{-3}$) may not be predicted in the location of any stations, as shown in this work (1-hr peak O_3 concentrations were 147 $\mu g\ m^{-3}$ and 127 $\mu g\ m^{-3}$ for measurements and simulations, respectively, at 1200 UTC for both values).

The European Directive 2002/3/EC[19] related to O_3 in ambient air establishes an uncertainty of 50% as the quality objective for modeling assessment methods. This uncertainty is defined as the maximum error of the measured and calculated concentration levels. In addition, the U.S. Environmental Protection Agency (EPA) has developed guidelines[20] for a min set of statistical measures to be used for these evaluations where monitoring data are sufficiently dense. Those statistical figures, considered in this work, are the mean normalized bias error (MNBE), the mean normalized gross error for concentrations above a prescribed threshold (MNGE), and the unpaired peak prediction accuracy (UPA). Observation-prediction pairs are excluded from the analysis if the observed concentration is below a certain cut-off; the cut-off levels vary from study to study, but often a level of 120 $\mu g\ m^{-3}$ is used,[21] which is the criterion applied in this work. Table 4 collects the results of both the discrete and categorical statistical analysis. Although there is no criterion set forth for a satisfactory model performance, the EPA[20] suggested values of ±10–15% for MNBE, +30–35% for the MNGE, and

Table 4. Statistical measures of model performance for 1 hr O_3 for the different nested configurations on August 15, 2000.

	EPA goal	Nested D1 (24 km)	Nested D2 (2 km)	Nested D3 (1 km)
Observed peak ($\mu g\ m^{-3}$)			147	
Modeled peak ($\mu g\ m^{-3}$)	—	97	111	127
UPA (%)	$<\pm$ 20	−33.8	−24.7	−13.8
MNBE (%)	$<\pm$ 15	−17.8	−19.1	−13.1
MNGE (%)	<35	19.3	19.6	13.6

±15–20% for the UPA to be met by modeling simulations of O_3 have been considered for regulatory applications.

The quality objective of an uncertainty of 50% for modeling assessment set by European legislation is less demanding than EPA standards and is achieved by simulations with every resolution considered (Table 4). An improvement in the unpaired peak accuracy is produced with an increase in resolution from the most coarse domain (D1) to the second nest (D2) and is indicated in the results (−33.80% to −24.7%, respectively). However, these values are not within the standard of ±15–20% set for the prediction of the peak; a finer resolution of 1 km (D3) is needed to meet this objective (−13.8%). The negative values for UPA in each nested domain indicate an underprediction in the simulated values with respect to the maximum measured peak in the domain of Tarragona (147 $\mu g\ m^{-3}$). For the MNBE, these indicators do not get better when increasing the resolution from 24 km in D1 to 2 km in D2 (values over the EPA standard of ±10–15% for normalized bias), but an important improvement is shown in the case of D3, where MNBE descends to −13.1%, meeting the aforementioned guidelines. The MNGE is met by all of the nested configurations (19.3%, 19.7%, and 13.6% for D1, D2 and D3, respectively), but results from D3 improve with respect to other nested configurations. Therefore, results indicate that a resolution of at least 1 km is needed when studying the phenomena of air pollution occurring in the very complex industrial area of Tarragona and to predict correctly the low-troposphere processes throughout a daily cycle. In addition, Lyons et al.[22] indicated that horizontal resolutions up to 1 km should be considered when simulating vertical motion of pollutants associated with sea breezes. Hence, a horizontal resolution of 1 km was selected for the study of the O_3 response to the emission controls of its precursors.

Description of Pollutants Dynamics for August 15, 2000 (Base Case)

The dynamics of the daily cycle of ground-level O_3 are depicted in Figure 4. The behavior of nocturnal flows in the D3 presents calm winds during nocturnal nights and the development of the sea breeze from 0800 UTC. The canalizations observed come conditioned because of the particular orography of the northern Mediterranean coast of the Iberian Peninsula. At night, the dominant reaction is the depletion of O_3 with the abundant nitrogen monoxide (NO) emissions in the industrial zone of Tarragona through the reaction $NO + O_3 \rightarrow NO_2 + O_2$, where O_3 oxidizes nitrogen monoxide, being consumed in the process.

Coastal mountain ranges in D3 promote the formation of anabatic winds from 0800 UTC. They help establishing the sea-breeze regime. At this time, mountain winds inland are well developed, helping the penetration of the breeze. Afterwards, the altitude of the mountain ranges hinders the advance of the sea breeze producing the accumulation of precursors; and the presence of solar radiation begins the formation of O_3. Orographic forcings undergone by the breeze front (reinforced by anabatic winds) contribute to the vertical injection of air masses with high levels of photochemical pollutants in this region to higher levels. As stated with lidar observations and simulations results,[5] these injections can be stressed with the convergence on mountain tops of the breeze front and anabatic winds of the northern slopes (Figure 5).

During the hours of photochemical activity, air masses act as photochemical reactors, where NO_x, VOCs, and solar radiation interact to form tropospheric O_3, peroxyacetylnitrate (PAN), and other photochemical pollutants. Afterwards, once the air masses overcome the mountain ranges, they are transported inland by the sea breeze, reinforced with anabatic winds, until they reach the area of Alcover, where the model provides values of 182 $\mu g\ m^{-3}$ of O_3 at 1200 UTC, exceeding the information threshold of 180 $\mu g\ m^{-3}$ set by Directive 2002/3/EC. Simultaneously, pollutants injected mechanically in a chimney effect are incorporated in return fluxes aloft that come toward the sea.[23–25] A fraction of these air masses are transported over the mixing layer out from the domain, extracting pollutants in a short-medium scale transport. The other fraction is forced to descend as a consequence of the compensatory subsidence over the eastern coast of the Iberian Peninsula[26] where they are recirculated and increase the levels of photochemical pollutants.

At 1400 UTC, winds overcome the coastal mountains, transporting pollutants inland toward the domain D2 (Figure 4). This situation remains similar until 2000 UTC, when the breeze weakens and turns toward the southwest in the coast, starting the development of the nocturnal land-breeze regime. This does not present intense draining, and the calm dominates the situation in plain areas. Katabatic winds are developed in the mountains; terral winds are reinforced by the katabatic winds of coastal mountains. During these hours the tropospheric

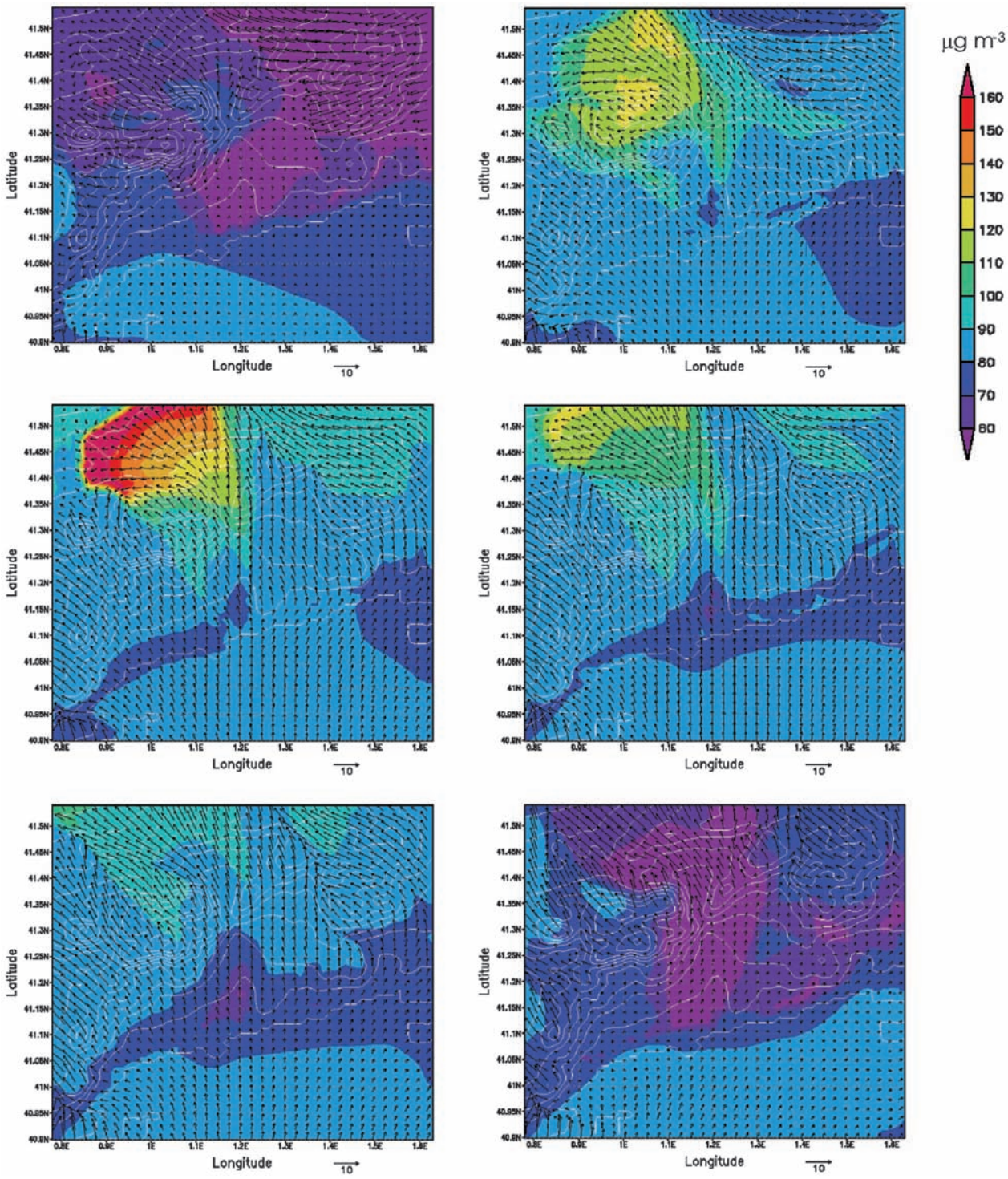

Figure 4. Wind vectors and O_3 concentrations ($\mu g\ m^{-3}$) in the domain of Tarragona (D3) at (from top-down and left-right) 0600 UTC, 1000 UTC, 1200 UTC, 1400 UTC, 1600 UTC and 2000 UTC.

O_3 is depleted because of the emissions of nitrogen oxides, as previously commented.

Effect of the Control of Emitter Sources on Photochemical Pollutants in the Area of Tarragona

Tropospheric O_3 is the most important photochemical pollutant in the area of Tarragona. Nevertheless, several species participate in the formation of O_3 and its chemistry and also in the air quality of D3. Therefore, to analyze the effects of the control of O_3 precursors, other species were also considered, such as NO_x, SO_2, NMVOCs, CO, nitric acid (HNO_3), PAN and total reactive nitrogen (NO_y).

The response of O_3 to the reduction of its precursors can be examined in additional detail if quantitative methods are used to define the chemistry of O_3-NO_x-VOCs. According to

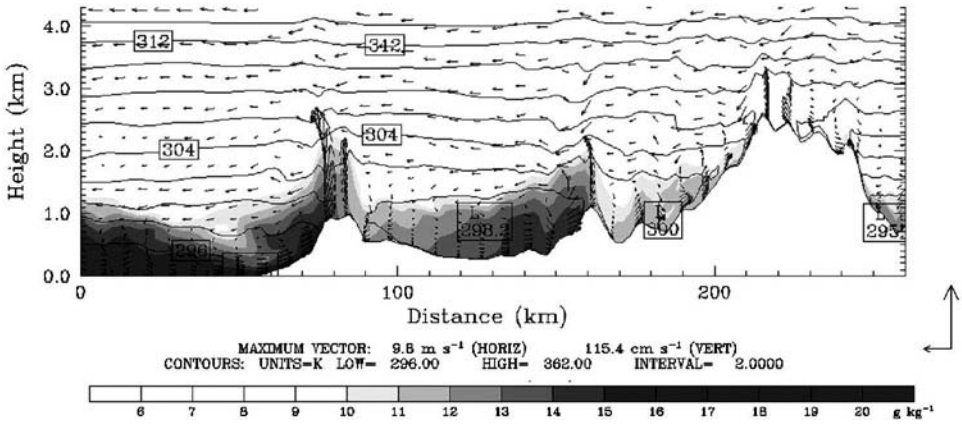

Figure 5. Vertical profile of the wind vectors, potential temperature, and mixing ratio for August 15, 2000 at 1100 UTC (Mediterranean Sea-Tarragona-Pyrenees profile).

Sillman et al.,[27] locations are defined as NO_x-sensitive for a specified hour if O_3 in the case with 35% reduced NO_x is lower than O_3 in both the base case and in the case with 35% reduced VOC by at least 4 $\mu g\ m^{-3}$ (2 ppb). Locations are classified as VOC-sensitive if the O_3 in the case with reduced VOC is lower than O_3 in the other cases by at least 4 $\mu g\ m^{-3}$. Locations that are neither VOC-sensitive or NO_x-sensitive by this definition are classified as having mixed sensitivity if O_3 in the cases with the reduced NO_x and with reduced VOC is lower than O_3 in the base case by at least 4 $\mu g\ m^{-3}$; locations are classified as insensitive to NO_x and VOC otherwise. These definitions are time-dependent; that is, a model location may be NO_x-sensitive at some times and VOC-sensitive at other times.

Jiménez and Baldasano[28] performed a sensitivity study for the NEIP, finding that at the time of maximum photochemical activity (1200 UTC), the industrial area of Tarragona increases its levels of O_3 when reducing total NO_x emissions 35%. On the other side, a reduction of 35% in total VOCs emissions causes an important diminution in the aforementioned area, and, thus, the authors indicated that this industrial area presents a VOC-sensitive chemistry during the hour of maximum O_3 formation.

Response of O_3 to Emission Controls

The results for different photochemical pollutants are summarized in Table 5 for peak levels for each of the seven scenarios proposed. The threshold of information

Table 5. Peak hourly values and percentage of reduction in domain D3 for different scenarios.

	Base Case	Scenario 1 Reduction 25% NO_x	Scenario 2 Reduction 25% VOCs	Scenario 3 Reduction 25% NO_x, VOCs	Scenario 4 Reduction 50% Traffic	Scenario 5 Reduction 100% Refinery	Scenario 6 Reduction 100% Biogenic
O_3 ($\mu g\ m^{-3}$)	182	201 ↑	161 ↓	179 ↓	181 ↓	189 ↑	181 ↓
NO_x ($\mu g\ m^{-3}$)	133	113 ↓	133	113 ↓	133	112 ↓	134 ↑
SO_2 ($\mu g\ m^{-3}$)	583	583	583	583	583	493 ↓	583
CO (ppb)	578	578	578	578	537 ↓	532 ↓	578
NMVOCs (ppm)	1.92	1.92	1.61 ↓	1.61 ↓	1.90 ↓	1.75 ↓	1.91 ↓
HNO_3 (ppb)	10.76	9.28 ↓	10.20 ↓	9.50 ↓	10.63 ↓	8.59 ↓	10.78 ↑
PAN (ppb)	3.15	3.78 ↑	2.54 ↓	3.03 ↓	3.09 ↓	3.44 ↑	3.03 ↓
NO_y (ppb)	100	83 ↓	98 ↓	82 ↓	99 ↓	81 ↓	100
Percentage of reduction respect to the base case							
O_3 (%)		10.2 ↑	−11.6 ↓	−2.0 ↓	−0.7 ↓	3.9 ↑	−0.9 ↓
NO_x (%)		−15.3 ↓	0.0	−15.6 ↓	−0.6 ↓	−16.0 ↓	0.1 ↑
SO_2 (%)		0.0	0.0	0.0	0.0	−15.3 ↓	0.0
CO (%)		0.0	0.0	0.0	−7.0 ↓	−7.9 ↓	0.0
NMVOCs (%)		0.1	−16.1 ↓	−16.0 ↓	−0.8 ↓	−8.9 ↓	−0.1 ↓
HNO_3 (%)		−13.8 ↓	−5.2 ↓	−11.7 ↓	−1.2 ↓	−20.1 ↓	0.2 ↑
PAN (%)		20.2 ↑	−19.4 ↓	−3.8 ↓	−1.7 ↓	9.2 ↑	−3.7 ↓
NO_y (%)		−16.9 ↓	−1.2 ↓	−17.6 ↓	−0.8 ↓	−18.9 ↓	0.0

Notes: ↑ = increment in the level of the pollutant respect to the base case; ↓ = diminution in the level of the pollutant respect to the base case.

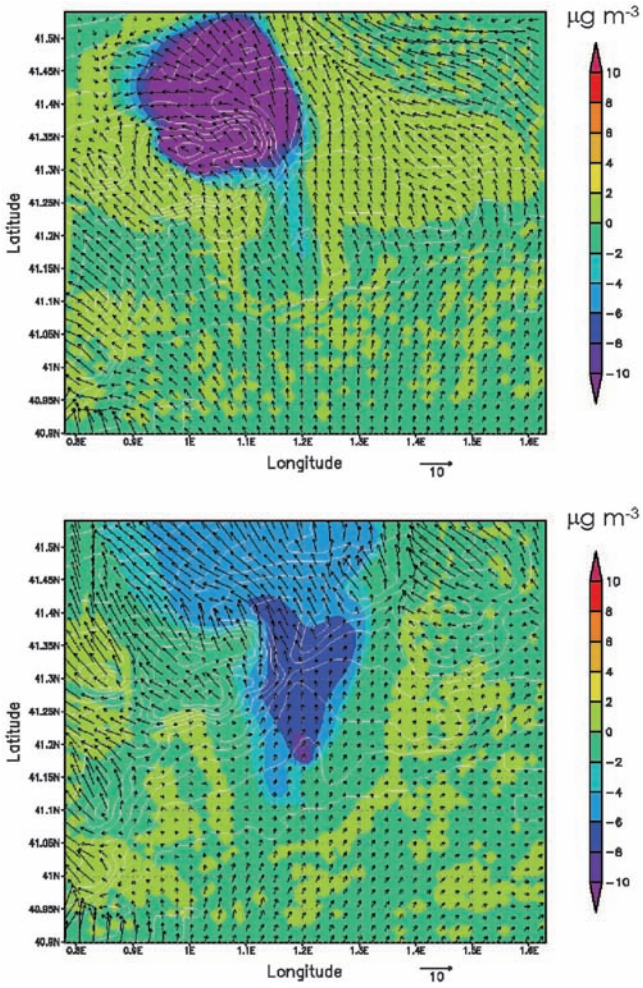

Figure 6. Difference between the base case and the scenario of reduction of industrial NO_x emissions (25%) at 1200 UTC (up) and 2000 UTC (down). A positive vale (red) indicates a reduction in the levels of O_3 in Scenario 2; a negative value (blue) indicates an increase in the levels of O_3 in Scenario 2 with respect to the base case.

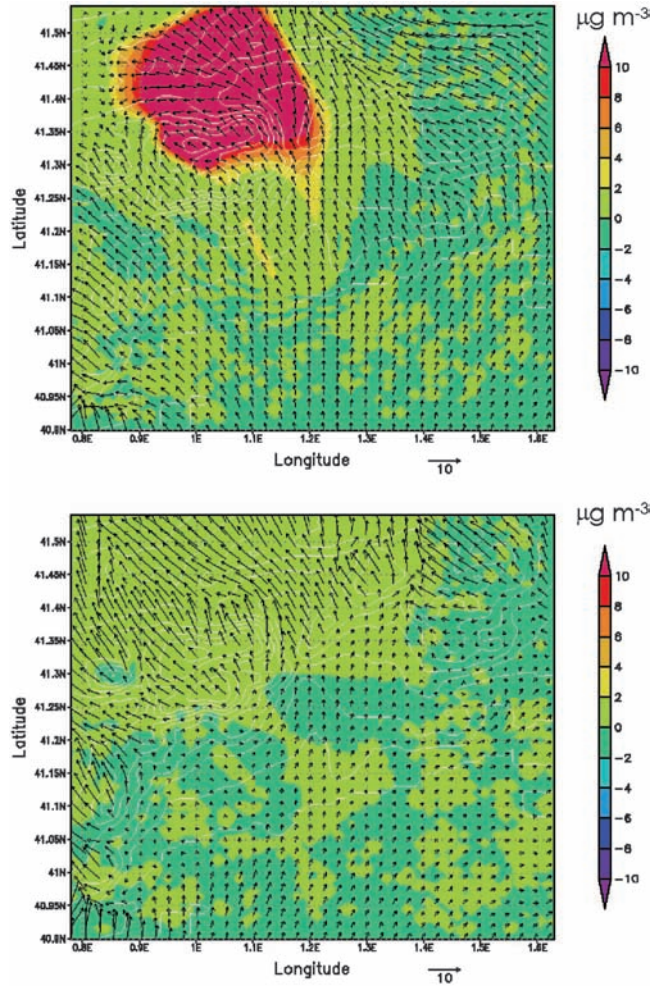

Figure 7. Difference between the base case and the scenario of reduction of industrial VOCs emissions (25%) at 1200 UTC (up) and 2000 UTC (down). A positive vale (red) indicates a reduction in the levels of O_3 in Scenario 3; a negative value (blue) indicates an increase in the levels of O_3 in Scenario 3 with respect to the base case.

(180 µg m^{-3}) set in Directive 2002/3/EC is achieved neither in the case of reducing the industrial emissions of VOCs by 25%, nor in the scenario where both NO_x and VOCs are reduced by 25%. Additionally, Table 5 shows the reduction percentages of peak concentrations for each scenario with respect to the base case.

Scenario 1: Reduction of Industrial NO_x Emissions (25%). Tables 4 and 5 and Figure 6 show that a reduction of 25% in the emissions of industrial NO_x represents an increase of 10% in the peak levels of tropospheric O_3 in D3 achieved at 1200 UTC (hour of maximum photochemical formation in this area), increasing O_3 levels from 182 µg m^{-3} for the base case to 201 µg m^{-3} in Scenario 1. This difference is principally observed downwind of the emission area (Alcover). Figure 6 also depicts that, at 2000 UTC, the lower industrial emissions of NO_x provoke an inferior destruction (or titulation) of tropospheric O_3 through the reaction $O_3 + NO \rightarrow NO_2 + O_2$.

Scenario 2: Reduction of Industrial VOCs Emissions (25%). In the case of reducing industrial VOCs emissions by 25%, a clear diminution of 12% is observed in the peak levels of tropospheric O_3 at 1200 UTC in D3 (Table 5), with concentrations reducing from 182 µg m^{-3} for the base case to 161 µg m^{-3} in Scenario 2 (Table 5 and Figure 7), with reductions of up to 20 µg m^{-3} in the downwind area of Alcover. With the results of Scenario 1 and 2, and according to the definition of sensitivity,[27] D3 undergoes a VOC-limited chemistry. Nocturnal chemistry is not altered by the reductions of VOCs, because organic compounds do not significantly contribute to night chemistry of O_3, and, therefore, no differences are observed.

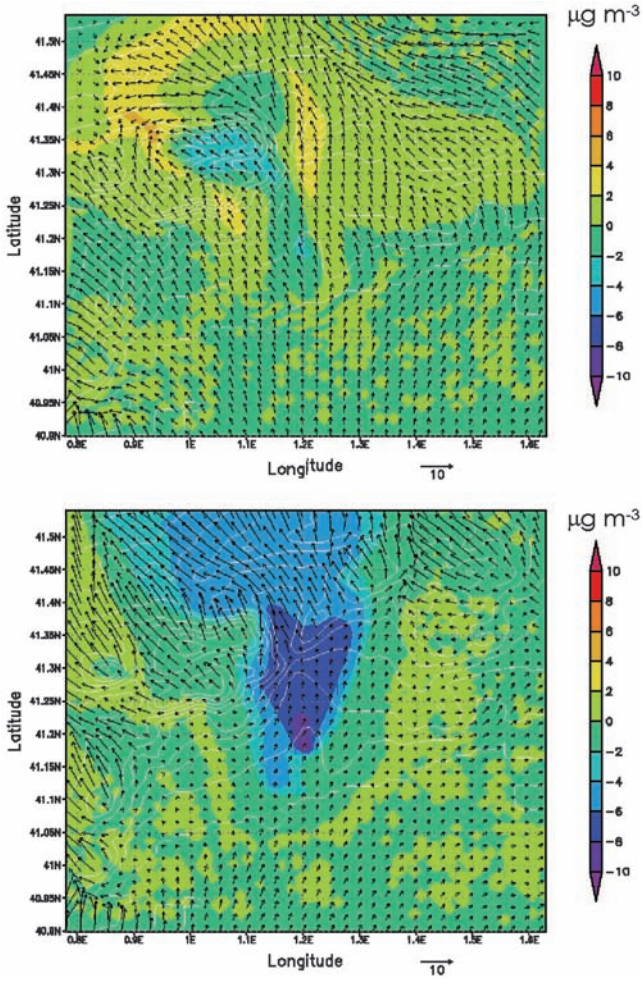

Figure 8. Difference between the base case and the scenario of reduction of industrial NO_x (25%) and VOCs emissions (25%) at 1200 UTC (up) and 2000 UTC (down). A positive vale (red) indicates a reduction in the levels of O_3 in Scenario 4; a negative value (blue) indicates an increase in the levels of O_3 in Scenario 4 with respect to the base case.

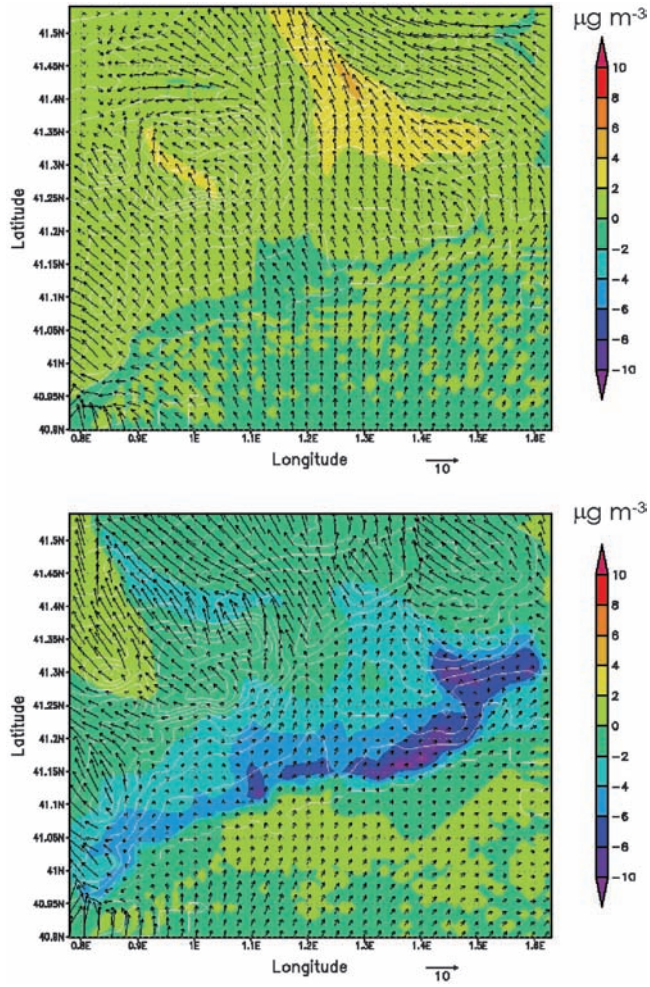

Figure 9. Difference between the base case and the scenario of reduction of on-road traffic emissions (50%) at 1200 UTC (up) and 2000 UTC (down). A positive vale (red) indicates a reduction in the levels of O_3 in Scenario 5; a negative value (blue) indicates an increase in the levels of O_3 in Scenario 5 respect to the base case.

Scenario 3: Reduction of Industrial NO_x (25%) and VOCs Emissions (25%). Simultaneous reductions of industrial NO_x and VOCs emissions lead to decreases of 3 $\mu g\ m^{-3}$ (Table 5 and Figure 8) in the domain of Tarragona, with 182 $\mu g\ m^{-3}$ in the base case and 179 $\mu g\ m^{-3}$ in Scenario 4, because this zone is strongly VOC limited. That represents a decrease of just 2% in peak levels of tropospheric O_3 at 1200 UTC (Table 5). At 2000 UTC, when photochemical activity ceases, the reduction in NO_x emissions provokes a lower titulation of tropospheric O_3, as commented before, allowing a higher accumulation of this photochemical pollutant and higher nocturnal levels.

Scenario 4: Reduction of On-Road Traffic (50%). This scenario intends to quantify the influence of road traffic in the levels of tropospheric O_3; therefore, a reduction of 50% in the total emissions from road traffic causes a diminution of peak O_3 levels of just 1 $\mu g\ m^{-3}$ (Figure 9) at 1200 UTC (reduction of 0.7%; Table 5). On the contrary, the impact on NO_x emissions is important, and, thus, night concentrations of O_3 at 2000 UTC are increased because of the lower destruction associated to lower ground-levels of nitrogen monoxide.

Scenario 5: Reduction of Emissions of Refinery (100%). The refinery is located in the D3 and represents a huge source of photochemical precursors and other pollutants, and, thus, it is interesting to remove the emissions from this refinery as a theoretical scenario. It should be considered that the uncertainty levels associated with the estimation of refinery emissions are particularly high;[7] therefore, results shown here are a primary approximation to the behavior of photochemical pollutants when removing the emissions of the refinery.

Results (Table 5) indicate that the peak O_3 level (189 $\mu g\ m^{-3}$) rises by 4% in the domain of study with respect to the levels of the base case, 182 $\mu g\ m^{-3}$ (increment of 7 $\mu g\ m^{-3}$). Scenario 5 presents a peculiar behavior, with a

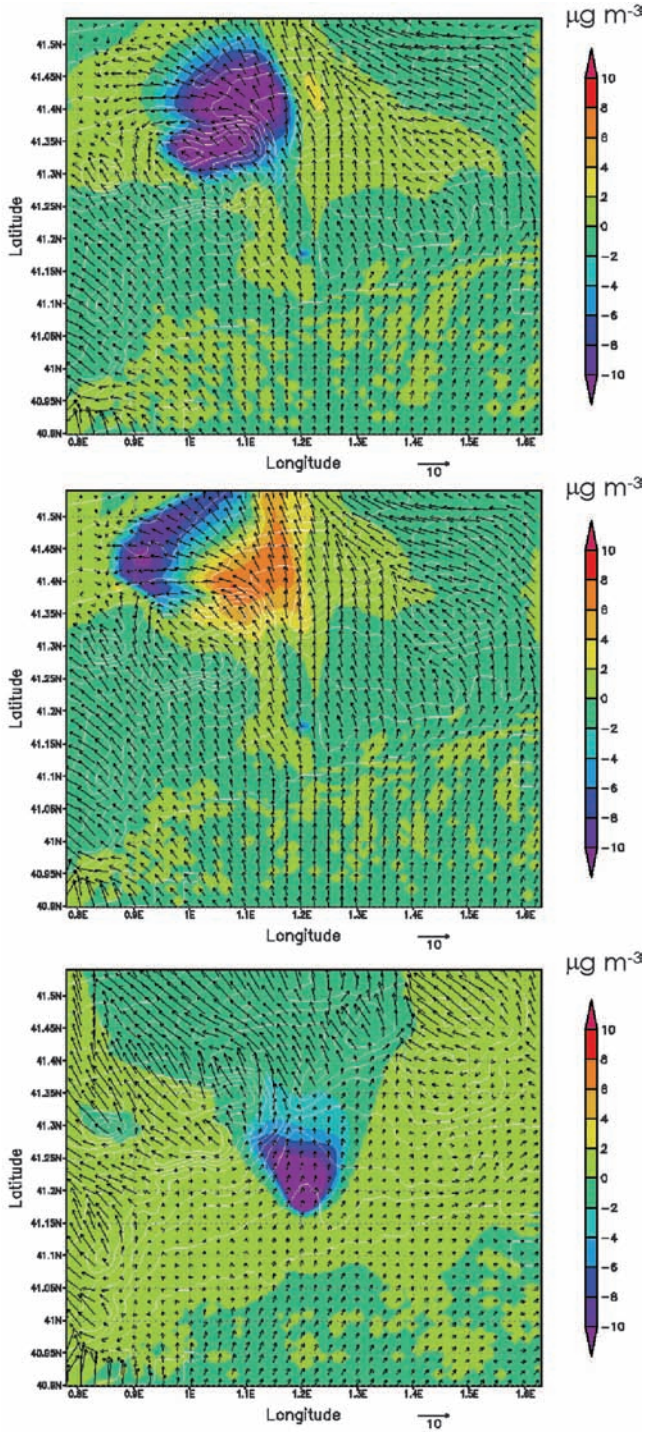

Figure 10. Difference between the base case and the scenario of reduction of refinery emissions (100%) at 1100 UTC (up), 1200 UTC (center), and 2000 UTC (down). A positive vale (red) indicates a reduction in the levels of O_3 in Scenario 6; a negative value (blue) indicates an increase in the levels of O_3 in Scenario 6 with respect to the base case.

change in the photochemical regime between 1100 and 1200 UTC (Figure 10). First, we would observe an increase in tropospheric O_3 levels as a consequence of the diminution of NO_x emissions, mainly if reduction of 100% in the emissions of this source is considered. Later, the aging

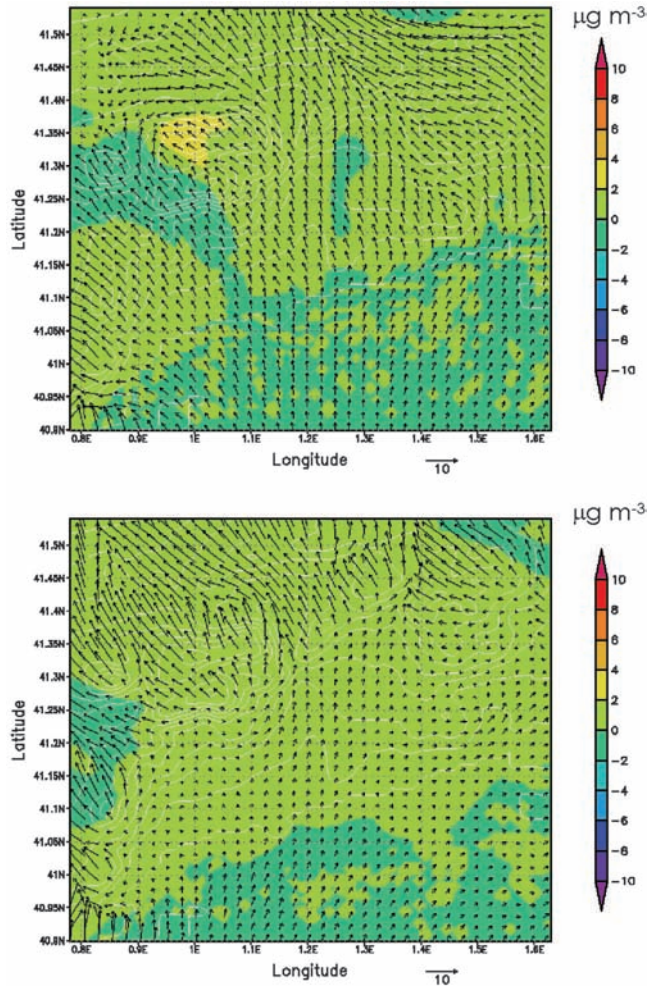

Figure 11. Difference between the base case and the scenario of reduction of biogenic emissions (100%) at 1200 UTC (up) and 2000 UTC (down). A positive vale (red) indicates a reduction in the levels of O_3 in Scenario 7; a negative value (blue) indicates an increase in the levels of O_3 in Scenario 7 with respect to the base case.

of the air mass promotes a diminution in photochemical formation and the transition of chemical regimes,[29] which is observed in D3 next to the coastal mountain range. At night (2000 UTC), the behavior is similar to Scenario 3, where both NO_x and VOCs are reduced, and the lack of nitrogen monoxide allows the accumulation and the increment of O_3.

Scenario 6: Reduction of Biogenic Emissions (100%). The last scenario responds to the necessity of quantifying the influence of biogenic emissions in the area of study. Biogenic emissions contribute mainly with VOCs (isoprene, terpenes, aldehydes, and paraffines). The high reactivity of biogenic species makes a significant contribution to atmospheric chemistry.[30] Those emissions may have a significant influence in the values of O_3.[31] In D3, Figure 11 shows that the contribution to its peak values is negligible because of the huge weight of industrial emissions in the area. Nevertheless, as shown in Table 5, it would

have a similar effect on O_3 as Scenario 4 (reduction of 50% of on-road emissions), with drops in O_3 concentrations of <1 μg m^{-3} (0.9% respect to base case) at the time of maximum photochemical formation, and they minimize during nighttime. Thus, the contribution of biogenic emissions to night chemistry is negligible.

Response of Other Photochemical Pollutants to Emission Controls

This section briefly depicts the response of other photochemical pollutants included in Table 5 in the different scenarios previously stated.

NO_x. O_3 concentrations are sensitive to NO and nitrogen dioxide (NO_2) concentrations and their reactions in the troposphere and also to the NO_2 photolysis rate and PAN formation and loss rates.[32] At the same time, the concentrations of NO_x play an essential role in the formation of nitrate radical and HNO_3.[3] Results indicate that higher reductions in ground-level NO_x are achieved in the case of removing the emissions from the refinery (133 μg m^{-3} in the base case versus 112 μg m^{-3} in Scenario 5, a 16% decrease). Similar reductions are presented when reducing NO_x emissions by 25% (113 μg m^{-3}, Scenarios 2 and 3). The control of traffic emissions has no implications in peak concentrations of NO_x within D3, which implies that this high concentration is because of industrial emissions. In all of the scenarios, NO_x levels are under the value of 200 μg m^{-3} set by European Directive 1999/30/EC as a maximum hourly value.[33]

NMVOCs. The presence of hydrocarbons is essential for the production of hydroxyl radicals, which are included in the cycle of formation of tropospheric O_3 and other photochemical oxidants as HNO_3 or PAN.[34] The reduction of 25% in the emissions of industrial VOCs produces reductions of 16% in the levels of NMVOCs (1.92 ppm in the base case and 1.61 ppm in Scenarios 2 and 3). Furthermore, the removal of the emissions from the refinery reduces the NMVOCs levels by 9% (1.75 ppm). Last, the control of on-road and biogenic emissions (Scenarios 5 and 6) has a minor influence on peak NMVOCs (reductions of ~1%).

SO_2. The role of SO_2 in atmospheric chemistry is related to acid rain and heterogeneous chemistry.[35] The high levels of this pollutant in D3 are mainly because of the refinery, as derived from EMICAT2000 and verified from simulations. The removal of this source decreases SO_2 ground levels by 15% (583 μg m^{-3} in base case versus 493 μg m^{-3} in Scenario 5); however, these levels are over the 1-hr threshold of 350 μg m^{-3} set in European Directive 1999/30/EC. The rest of the scenarios do not show noteworthy variations regarding the base case.

CO. The atmospheric oxidation of carbon monoxide (CO) in the presence of the hydroxyl radical can be viewed as a catalytic oxidation of CO to CO_2 with the formation of a molecule of O_3.[36] The scenarios that undergo more important reductions in CO levels with respect to the base case (578 ppb) are Scenario 4 (reduction of 50% of on-road traffic, 537 pbb) and Scenario 5 (reduction of 100% of refinery emissions, 532 ppb). These cuts in ground levels represent a reduction of 7% and 8%, respectively. In the rest of the scenarios, maximum concentrations of CO are not observed.

HNO_3. The majority of HNO_3 produced in all of the simulations during daylight hours is through the OH + NO_2 → HNO_3 reaction, which is one of the most important daytime reactions affecting tropospheric O_3.[35] Therefore, the formation of HNO_3 is not only related to the presence of NO_2, but also in the radical amount (in the formation of which NMVOCs participate). The base case levels of HNO_3 are 10.76 ppb, and important reductions in its levels are obtained when controlling industrial emissions of NO_x (because of the diminution of NO_2), VOCs (reduction of OH radicals), and both NO_x and VOCs. The most favorable scenario is the reduction of 100% in the emissions from the refinery, where peak concentrations of HNO_3 are reduced by 20% (8.59 ppb of HNO_3). The reduction of traffic does not significantly affect the concentrations of this pollutant; meanwhile, the removal of biogenic emissions in D3 slightly raises the levels of HNO_3.

PAN. PAN has long been known to be an important atmospheric species. It acts as a reservoir for NO_x and acetyl peroxy radicals (C_2O_3).[37] PAN and analogues are formed during degradation of aldehydes by the reaction of alkyl and acyl peroxy radicals with NO_2. The thermal decomposition of PAN leads to the formation of CO_2, NO_2, and peroxy radicals. In turn, the reactions of peroxy radicals lead to production of HO_2 and formaldehyde, which contribute to photochemical reactions including O_3 formation.

Variations of PAN are related to those of O_3;[38] therefore, in a VOCs-limited regime, a reduction of NO_x would lead to an increase of PAN levels. A control in the levels of VOCs improves the problems related to this photooxidant. Base case concentrations reach 3.15 ppb, which would increase to 3.78 and 3.44 in Scenario 1 (reduction of 25% in industrial NO_x) and Scenario 5 (removal of the refinery), respectively. These variations imply increments

of 20% and 9%, with the base case as reference. A reduction is observed in the case of controlling industrial VOCs (19%, 2.54 ppb) and when controlling simultaneously NO_x and VOCs emissions (4%, 3.03 ppb). At the same time, concentrations of PAN would drop by 4% if removing biogenic emissions, because they are an important source of aldehydes,[9] of which the degradation by OH radicals actively participates, and the generation of peroxy acetyl radical leads to PAN and its derivates.[39] The control of traffic emissions would only reduce the levels of this photooxidant on a 2%.

Total NO_y. NO_y is the sum of the ground-level concentration of nitrogen oxides and all of the nitrogen oxidation products by organic species. This is a good indicator of the sensitivity to NO_x and VOCs, because NO_y is related to the balance of both species within an air mass and allows us to have a global idea of the control of precursors.[28] For this species, all of the scenarios (except removal of biogenic emissions) lead to diminutions with respect to the base case (100 ppb). The most relevant case is the reduction by 100% of the emissions of the refinery that limits both NO_x emissions and the oxidation of nitrogen because of the reduction of VOCs. In this scenario, NO_y ground levels drop off to 81 ppb (reduction of 19%). The control of the industrial NO_x emissions is effective (83 ppb, reduction of 17%) as is the control of both industrial NO_x and VOCs emissions (82 ppb, reduction of 18%). On-road traffic reduction and the control of industrial VOCs emissions lead to drops in NO_y levels of ~1%.

CONCLUSIONS

A multiscale-nested approach was applied to simulate photochemical pollution in very complex terrains, as the NEIP (D2), and, more specifically, the industrial domain of Tarragona (D3). Results indicate that a very high-resolution grid (1 km) and a time resolution of 1 hr is needed when describing the dynamics of O_3 and other photochemical pollutants and also to achieve the goals for model performance established by the EPA and the European Legislation.

According to the Gothenburg Protocol and Directive 2001/81/EC, different scenarios have been set to establish hypothetical control policies for the emissions of O_3 precursors in the industrial area of Tarragona. The O_3 chemistry in the industrial domain of Tarragona is strongly sensitive to VOCs, and, therefore, the high levels of O_3 in the area are controlled by the industrial emissions of VOCs. At the same time, the contribution of on-road traffic and biogenic emissions in the area is much lower than the weight of industrial sources, except in the case of CO. For this pollutant, traffic plays a determinant role in maximum levels. The higher percentages of reduction for ground-level O_3 are achieved when reducing by 25% the emissions of industrial VOCs. On the contrary, reductions in the industrial emissions of NO_x contribute to a strong increase in hourly maximum concentrations of ground-level O_3. The same behavior is observed in Scenario 5 (no refinery); the rest of the scenarios do not show important variations respect to the base case.

Although results indicate that the control of industrial NO_x emissions (alone or combined with reductions of VOCs) contributes to the increment of tropospheric O_3 concentrations, the reduction in the emissions of this primary pollutant is effective in the improvement of air quality related to ground levels of NO_x, HNO_3 (related to organic nitrogen, which participates in the formation of secondary aerosols), and total NO_y.

Scenario 5 (D3 with no refinery) deserves a special analysis, because the refinery is responsible for a high percentage of the emissions of primary pollutants (NO_x, VOCs, SO_2, and CO) in the area of Tarragona. The improvement of air quality related to CO and SO_2 is noticeable; nevertheless, it is also an important source of NO_x that, when removed in VOCs-limited domains, produces a small increase in tropospheric O_3 concentrations.

The study of the different scenarios included in this work indicates that air quality modeling could be a useful tool to evaluate the chemical sensitivity of the system O_3-NO_x-VOCs when establishing policies of emissions controls from different emission sources. However, we should bear in mind that the regimes of chemical sensitivity vary with the hour of the day, changes from event to event, and with location within a same domain.

The practical implementation of these results is not an easy task, because it involves not only environmental policies but also socioeconomic parameters that are difficult to quantify. In addition, the impact of different policies in the diverse pollutants magnifies the difficulty of setting global policies.

ACKNOWLEDGMENTS

This work was developed under the research contract REN2003-09753-C02 of the Spanish Ministry of Science and Technology. The Spanish Ministry of Education is also thanked for the Formación de Profesorado Universitario doctoral fellowship held by Pedro Jiménez. The authors thank Oriol Jorba for providing meteorological fields and Eugeni López for the implementation of EMICAT2000 into a GIS system. Air quality stations data and information for implementing industrial emissions were provided by the Environmental Department of the Catalonia Government (Spain).

REFERENCES

1. Jiménez, P.; Jorba, O.; Baldasano, J.M. Influence of Horizontal Model Grid Resolution on Tropospheric Ozone Levels. In *Harmonisation 2004*, Proceedings of the 9th International Conference on Harmonisation within Atmospheric Dispersion Modelling for Regulatory Purposes, Garmish-Partenkircher, Germany, June 1–4, 2004; Forschungszentrum Karlsruhe GmbH: Karlsruhe, Germany, 2004; pp 219–223.
2. Kessler, Ch., Brücher, W.; Memmesheimer, M.; Kerschgens, M.; Ebel, A. Simulation of Air Pollution With Nested Models in North Rhine-Westphalia; *Atmos. Environ.* **2001**, *35,* Suppl.1:S3–S12.
3. Atkinson, R. Atmospheric Chemistry of VOCs and NO_x; *Atmos. Environ.* **2000**, *34,* 2063-2101.
4. Sillman, S. The Relation Between Ozone, NO_x and Hydrocarbons in Urban and Polluted Rural Environments; *Atmos. Environ.* **1999**, *33,* 1821-1845.
5. Pérez, C.; Sicard, M.; Jorba, O.; Comerón, A.; Baldasano, J.M. Summertime Re-Circulations of Air Pollutants Over the North-Eastern Iberian Coast Observed From Systematic EARLINET Lidar Measurements in Barcelona; *Atmos. Environ.* **2004**, *38,* 3983-4000.
6. Jorba, O.; Pérez, C.; Rocadenbosch, F.; Baldasano, J.M. Cluster Analysis of 4-day Back Trajectories Arriving in the Barcelona Area (Spain) From 1997 to 2002; *J. Applied Meteorol.* **2004**, *6,* 887-901.
7. Parra, R. Development of the EMICAT 2000 Model for the Estimation of air Pollutants Emissions in Catalonia and Its Use in Photochemical Dispersion Models. Ph.D. Dissertation (in Spanish), Polytechnic University of Catalonia, Catalonia, Spain, July 2004. Available at http://www.tdx.cesca.es/TDX-0803104–102139 (accessed June 23, 2005).
8. *PSU/NCAR Mesoscale Modeling System Tutorial Class Notes and User's Guide: MM5 Modeling System Version 3*. Mesoscale and Microscale Meteorology Division, National Center for Atmospheric Research: Boulder, CO; 2001. Available at http://www.mmm.ucar.edu/mm5/documents/tutorial-v3-notes-pdf/tutorial.cover.pdf (accessed June 23, 2005).
9. Parra, R.; Gassó, S., Baldasano, J.M. Estimating the Biogenic Emissions of Non-Methane Volatile Organic Compounds from the Northwestern Mediterranean Vegetation of Catalonia, Spain; *Sci. Total Environ.* **2004**, *329,* 241-259.
10. Ntziachristos, L.; Samaras, Z. *COPERT III Computer Programme to Calculate Emissions from Road Transport. Methodology and Emission Factors (Version 2.1)*; European Environment Agency, Technical report No 49, 2000.
11. Parra, R.; Baldasano, J.M. Modelling the On-Road Traffic Emissions from Catalonia (Spain) for Photochemical Air Pollution Research. Weekday-Weekend Differences. In *Proceedings of the 12th International Conference on Air Pollution (AP'2004)*. Rhodes Greece, 2004; C.A. Brebbia, Wessex Institute of Technology: Southampton, UK, 2004; pp 3–12.
12. Byun, D.W., Ching, J.K.S., Eds. *Science Algorithms of the EPA Models-3 Community Multiscale Air Quality (CMAQ) Modeling System*. EPA Report N. EPA-600/R-99/030, Office of Research and Development. U.S. Environmental Protection Agency: Washington, DC, 1999.
13. Berge, E.; Huang, H-C.; Chang, J.; Liu, T-H. A Study of the Importance of Initial Conditions for Photochemical Oxidant Modeling; *J. Geophys. Res.* **2001,** *106,* 1347-1363.
14. Jiménez, P.; Dabdub, D.; Baldasano, J.M. Comparison of Photochemical Mechanisms for Air Quality Modeling; *Atmos. Environ.* **2003**, *37,* 4179-4194.
15. Gery, M.W.; Whitten, G.Z.; Killus, J.P.; Dodge, M.C. A Photochemical Kinetics Mechanism for Urban and Regional Scale Computer Modeling; *J. Geophys. Res.* **1989,** *94,* 12925-12956.
16. Huang, H-C., Chang, J.S. On the Performance of Numerical Solvers for a Chemistry Submodel in Three-Dimensional Air Quality Models; *J. Geophys. Res.* **2001**, *106,* 20175-20188.
17. Directive 2001/81/EC of the European Parliament and of the Council of 23 October 2001 on National Emission Ceilings for Certain Atmospheric Pollutants; *Official Journal L 209*, 27/11/2001; European Union: Brussels, Belgium; pp 22–30.
18. *Atmospheric Emissions in Catalonia. A quantitative Approach (In Catalan)*. Quaderns de Medi Ambient. Número 5. Generalitat de Catalunya: Barcelona, Spain, 1996; p 16.
19. Directive 2002/3/EC of the European Parliament and of the Council of 12 February 2002 Relating to Ozone in Ambient Air. *Official Journal L 67*, 9/3/2002; European Union: Brussels, Belgium; pp 14–30.
20. *Guideline for Regulatory Application of the Urban Airshed Model*. US EPA Report No. EPA-450/4–91-013. U.S. Environmental Protection Agency, Office of Air and Radiation, Office of Air Quality Planning and Standards, Technical Support Division: Research Triangle Park, NC, 1991.
21. Hogrefe, C.; Rao, S.T.; Kasibhatla, P.; Hao, W.; Sistla, G.; Mathur, R.; McHenry, J. Evaluating the Performance of Regional-Scale Photochemical Modeling Systems: Part II-Ozone Predictions; *Atmos. Environ.* **2001**, *35,* 4175-4188.
22. Lyons, W.A.; Pielke, R.A.; Tremback, C.J.; Walko, R.L.; Moon, D.A.; Keen, C.S. Modeling the Impacts of Mesoscale Vertical Motions Upon Coastal Zone air Pollution Dispersion; *Atmos. Environ.* **1995**, *29,* 283-301.
23. Baldasano, J.M., Cremades, L., Soriano, C. Circulation of air pollutants over the Barcelona geographical area in summer. In *Proceedings of Sixth European Symposium Physico-Chemical Behavior of Atmospheric Pollutants*. Varese, Italy, 18–22 October, 1993. Report EUR 15609/1 EN, 1994, pp 474–479.
24. Millán, M.M., Artiñano, B., Alonso, L., Castro, M., Fernandez-Patier, R., Goberna, J. *Mesometeorological Cycles of Air Pollution in the Iberian Peninsula. Air Pollution Research Report 44*. Commission of the European Communities: Brussels, Belgium, 1992; p 219.
25. Millán, M.M.; Salvador, R.; Mantilla, E. Photooxidant Dynamics in the Mediterranean Basin in Summer: Results from European Research Projects; *J. Geophys. Res.* **1997,** *102,* 8811-8823.
26. Millán, M.M.; Salvador, R.; Mantilla, E.; Artíñano, B. Meteorology and Photochemical Air Pollution in Southern Europe: Experimental Results from EC Research Projects; *Atmos. Environ.* **1996**, *30,* 1909-1924.
27. Sillman, S., Vautard, R. Menut, L., Kley, D. 2003. O_3-NO_x-VOC Sensitivity and NO_x-VOC Indicators in Paris: Results from Models and Atmospheric Pollution over the Paris Area (ESQUIF) Measurements; *J. Geophys. Res.* **2003**, *108,* 8563.
28. Jiménez, P.; Baldasano, J.M. Ozone Response to Precursor Controls in Very Complex Terrains: Use of Photochemical Indicators to Assess O_3-NO_x-VOC Sensitivity in the Northeastern Iberian Peninsula; *J. Geophys. Res.* **2004**, *109,* 4985.
29. Dommen, J.; Prevot, A.S.H.; Hering, A.M.; Staffelbach, T.; Kok. G.L.; Schillawski, R.D. Photochemical Production and Aging of an Urban Air Mass; *J. Geophys. Res.* **1999,** *104,* 5493-5506.
30. Atkinson, R.; Arey, J. Atmospheric Chemistry of Biogenic Organic Compounds; *Accounts of Chemical Research* **1998**, *31,* 574-583.
31. Sollmon, F.; Sarrat, C.; Serca, D.; Tulet, P.; Rosset, R. Isoprene and Monoterpenes Biogenic Emissions in France: Modelling and Impact During a Regional Pollution Episode; *Atmos. Environ.* **2004**, *38,* 3853-3865.
32. Gao, D.; Stockwell, W.R.; Milford, J.B. Global Uncertainty Analysis of a Regional-Scale Gas-Phase Chemical Mechanism; *J. Geophys. Res.* **1996**, *101,* 9107-9119.
33. Council Directive 1999/30EC of 22 April 1999 Relating to Limit Values for Sulphur Dioxide, Nitrogen Dioxide and Oxides of Nitrogen, Particulate Matter and Lead in Ambient Air. *Official Journal L* 163, 39/6/2001, European Union: Brussels, Belgium, 1999; pp 41–60.
34. Luecken, D.J.; Tonnesen, G.S.; Sickles, J.E. Differences in NO_y Speciation Predicted by Three Photochemical Mechanisms; *Atmos. Environ.* **1999**, *33,* 1073-1084.
35. Seinfeld, J.H., Pandis, S.N. *Atmospheric Chemistry and Physics: from Air Pollution to Climate Change*. John Wiley & Sons, New York, NY, 1998; p 1326.
36. Wayne, R.P. *Chemistry of Atmospheres*. 3rd ed. Oxford University Press: Oxford, UK, 2000; p 775.
37. Stockwell, W.R.; Milford, J.B.; Gao, D.; Yang, Y.J. The Effect of Acetyl Peroxy-Peroxy Radical Reactions on Peroxyacetyl Nitrate and Ozone Concentrations; *Atmos. Environ.* **1995**, *29,* 1591-1599.
38. Grosjean, E.; Grosjean, D.; Woodhouse, L.F. Peroxyacetyl Nitrate and Peroxypropionyl Nitrate During SCOS 97-NARSTO; *Environ. Sci. Technol.* **2001**, *35,* 4007-4014.
39. Aschmann, S.M.; Arey, J.; Atkinson, R. OH Radical Formation From the Gas-Phase Reactions of O_3 with a Series of Terpenes; *Atmos. Environ.* **2002**, *36,* 4347-4355.

About the Authors

Pedro Jiménez and René Parra are post-doctoral researchers from the Laboratory of Environmental Modeling, and José M. Baldasano is a full professor of Environmental Engineering and head of the Laboratory of Environmental Modeling, Universitat Politècnica de Catalunya. Address correspondence to: José M. Baldasano, Laboratory of Environmental Modeling, Universitat Politècnica de Catalunya, Avda. Diagonal 647 10.23, 08028 Barcelona, Spain; phone: 34-934011744; fax: 34-93340255; e-mail: jose.baldasano@upc.edu.